Available online at www.sciencedirect.com
SCIENCE DIRECT®
Journal of the European Ceramic Society 25 (2005) 1183–1189
www.elsevier.com/locate/jeurceramsoc

Order–disorder behaviour in $0.9Ba([Zn_{0.60}Co_{0.40}]_{1/3}Nb_{2/3})O_3$–$0.1Ba(Ga_{0.5}Ta_{0.5})O_3$ microwave dielectric resonators

I. M. Reaney [a,*], Y. Iqbal [a], H. Zheng [a], A. Feteira [a], H. Hughes [b], D. Iddles [b], D. Muir [b], T. Price [b]

[a] *Department of Engineering Materials, University of Sheffield, Sheffield S1 3JD, UK*
[b] *Filtronic Comtek, Ceramics Division, Enterprise Drive, Four Ashes, Wolverhampton WV10 7DB, UK*

Received 8 June 2003; received in revised form 1 December 2003; accepted 7 December 2003
Available online 10 July 2004

Abstract

$0.9Ba([Zn_{0.60}Co_{0.40}]_{1/3}Nb_{2/3})O_3$–$0.1Ba(Ga_{0.5}Ta_{0.5})O_3$ (BCZN–BGT) ceramic resonators (quality factor, $Q = 32{,}000$ at the rate of 3.05 GHz, relative permittivity, $\varepsilon_r = 35$ and temperature coefficient of the resonant, $\tau_f = 0$) have been fabricated which are suitable in terms of cost and performance for base stations supporting third generation architecture. The new compounds are perovskite structured ($a = 4.09$ Å) but exhibit no superlattice reflections at any heat treatment temperature according to X-ray diffraction (XRD). However, annealing and quenching of samples followed by transmission electron microscopy and Raman spectroscopy revealed an order–disorder phase transition at ~1200 °C. Annealing below this temperature (1100 °C) gave rise to discrete $\pm 1/3\{h\,k\,l\}_p$ and diffuse $1/2\{h\,k\,l\}_p$ superlattice reflections in the same $\langle 1\,1\,0\rangle_p$ zone axis electron diffraction patterns and the presence of F_{2g} and A_{1g} modes in Raman spectra. It is proposed that $\pm 1/3\{h\,k\,l\}_p$ reflections result from 1:2 long-range ordered domains of BCZN whereas the diffuse $1/2\{h\,k\,l\}_p$ reflections arise from short range fcc ordered BGT rich regions at the 1:2 domain boundaries. A short-range ordered fcc superlattice was observed in samples quenched from above the order–disorder phase transition (>1200 °C) which was accompanied by the presence of only the A_{1g} mode in Raman spectra.

Keywords: Microwave dielectrics; Perovskites; Ordering; Superlattice; Transmission electron microscopy; Raman spectroscopy; $Ba(Ga,Ta)O_3$; $Ba(Zn,Co,Nb)O_3$

1. Introduction

Low loss dielectric ceramics with medium permittivities ($\varepsilon_r = 25$–50) are the materials of choice for mobile phone base station technology where they act as filters, resonators and tuners.[1] Currently, ceramics based on the solid solutions $CaTiO_3$–$NdAlO_3$[2] and $ZrTiO_4$–$ZnNb_2O_6$[3] are the market leaders in these applications and typically commercial pucks have $\varepsilon_r \approx 43$–45, quality factor, $Q \approx 25{,}000$ at the rate of 2 GHz and temperature coefficient of the resonant frequency, $\tau_f = \pm 3$. Where selectivity for a given resonant frequency (f_0) and optimisation of bandwidth are paramount, filter designers would prefer to use 1/3:2/3 complex perovskite compositions derived from $Ba(Zn_{1/3}Ta_{2/3})O_3$ (BZT)[4] and $Ba(Mg_{1/3}Ta_{2/3})O_3$ (BMT)[5] due to their higher Q-values (≥70,000 at the rate of 2 GHz). Unfortunately, Ta_2O_5 is expensive and the cost per resonator puck of BZT is too great for the expected mass market for third generation mobile systems. Nb_2O_5 is isostructural with Ta_2O_5 and Nb^{5+} and Ta^{5+} have identical ionic radii (0.64 Å) and electronic structures.[6] Therefore, Nb_2O_5 is a logical substituent for Ta_2O_5 in complex perovskite compositions. Compounds such as $BaZn_{1/3}Nb_{2/3}O_3$ (BZN), for which $\varepsilon_r = 38$, $\tau_f = +40$ and $Q \times f_o = 60{,}000$ GHz, show promise as a basis for the development of MW dielectrics.[7–9] Until recently, however, problems have been encountered in achieving zero τ_f and optimising and controlling Q. In 2001, Hughes et al.[10] reported on the composition $0.9Ba([Zn_{0.60}Co_{0.40}]_{1/3}Nb_{2/3})O_3$–$0.1Ba(Ga_{0.5}Ta_{0.5})O_3$ (BCZN–BGT) for which $\tau_f = 0$, $\varepsilon_r = 35$ and $Q = 32{,}000$

* Corresponding author. Tel.: +44-114-222-5471; fax: +44-114-222-5943.
E-mail address: I.M.Reaney@sheffield.ac.uk (I.M. Reaney).

0955-2219/$ – see front matter © 2004 Elsevier Ltd. All rights reserved.
doi:10.1016/j.jeurceramsoc.2003.12.018

at the rate of 3.05 GHz ($Q \times f_o = 100{,}000$ GHz). Moreover, it was demonstrated that compositions could be scaled up to form cylindrical resonator pucks with outer and inner diameters of 27 and 10.4 mm, respectively, for which $Q \times f_o = 98{,}000$ GHz.[10]

Although technologically this compound was an important advance in the fabrication of ceramic resonators for mobile systems, little is known about its crystal chemistry and microstructure. For example, Hughes et al.[10] reported that it appeared disordered by X-ray diffraction (XRD) but the scattering power difference between Zn/Co and Nb is small compared with that between, e.g. Zn and Ta ions in BZT-based compounds. Detection of ordering in BCZN is therefore difficult and it remains an open question if or at what temperature the compound undergoes an order–disorder phase transition.

Many powder XRD and transmission electron microscopy (TEM) studies have been performed on Ba-based complex perovskites and it has been known since the late 1970s that the degree of order in, e.g. BZT, increases on annealing typically between 1400 and 1500 °C.[11,12] Moreover, it is now well established that an increase in the degree of order results in an increased Q.[12] In the late 1990s, Reaney et al.[13] reported that the order–disorder phase transition temperature in pure BZT was between 1600 and 1650 °C and was reversible. A high degree of order coupled with large ordered domains could be obtained by annealing at 1600 °C but this was accompanied by large scale ZnO loss. In a more recent publication, Reaney et al.[14] investigated $0.95BaZn_{1/3}Ta_{2/3}O_3$–$0.05SrGa_{1/2}Ta_{1/2}O_3$ (BZT–SGT)[15] commercial resonator pucks, identifying an order–disorder phase transition at ~1500 °C. These authors also suggested that BZT–SGT ceramics should be sintered at 1525 °C/2 h (above the order–disorder transition) followed by annealing 24 h at 1275 °C in air. This schedule maximised density and the degree of order but minimised ZnO loss and resulted in the highest reported Q values for BZT-based commercial resonators ($Q = 79{,}000$ at the rate of 2 GHz). Similar results have been obtained on $BaZn_{1/3}Ta_{2/3}O_3$–$BaZrO_3$ (BZT–BZ) ceramics by Davies and Tong[9] who also demonstrated the strong link between ordering and Q and observed that, at a sintering temperature of 1510 °C, increasing the $BaZrO_3$ concentration from 3 to 5 mol% resulted in a switch from long range 1:2 to short range 1:1 ordering. This was accompanied by a decrease in the sintering time at temperature to achieve optimum Q. In light of more recent studies,[13,14] it seems likely that the 1:2 long-range ordered phase transition temperature in BZT–BZ was suppressed to below 1510 °C as BZ concentration increased since the electron diffraction data obtained as a function of composition were similar to those obtained as a function of temperature by Reaney et al. in pure BZT[13] and BZT–SGT[14].

In contrast, comparatively little is known on structure–property relations in BZN or BCN based compounds. Noh et al.[16] sintered BZN over a range of temperatures and concluded that the grain size and the density were more important in controlling Q than the degree of 1:2 order. Ahn et al.[17] investigated BCN and observed that, although long range 1:2 order was present in samples sintered at 1400 °C, at 1450 °C, the intensities of the $\pm 1/3\{h\,k\,l\}$ reflections in electron diffraction patterns became weaker and more diffuse and XRD revealed a reduction in the total degree of order. Endo et al.[18] substituted Co for Zn on the B-site and succeeded in producing a zero τ_f high Q ($Q \times f_o = 70{,}000$ at the rate of 6.5 GHz) composition. The degree of order, however, was not studied and control of the valence state of Co was reported as difficult and blamed for the poor reproducibility of the Q values. It should be noted that compositions of Endo et al.[18] were produced as small 1–2 cm test pieces and measured at high frequencies (6.5 GHz). Although $Q \times f_o$ was reported as a 70,000 GHz, this would not be easily reproduced in 2–3 GHz resonator pucks since larger ceramics contain more defects and $Q \times f_o$ is not constant as widely reported.[19] Colla et al.[20] investigated BZN–$SrZn_{1/3}Nb_{2/3}O_3$ solid solutions as a test case to study the changes in τ_f as a function Sr concentration in complex perovskites. They concluded that the substitution of Sr for Ba resulted in the onset of a series of phase transition, involving rotations of the O-octahedra, which controlled the magnitude and sign of τ_f.

In this investigation, a series of quenching experiments are performed to ascertain the approximate temperature of the order–disorder phase transition in BCZN–BGT. The structure and microstructure of the ordered and disordered phases are investigated using XRD, TEM and Raman spectroscopy.

2. Experimental

2.1. Ceramic processing

Standard electronic grade purity raw materials (>99.5%) with a d_{50} of approximately 1–3 μm were batched in lots of 100–200 kg. Measurement accuracy for the individual powders were maintained to 0.002 kg. The powders were transferred to an attrition mill and milled for approximately 3 h with deionised water and YSZ media. Milling was complete after 3 h and the d_{50} of the mix was below 3 μm. After spray drying the powder was calcined in a 1000 l furnace for 10 h at 1250 °C. Post calcination, the powders were re-milled in the attrition mill until the d_{50} of the slip was below 5 μm. Binders at the rate of 2 wt.% were subsequently added and the slip spray dried. Spray dried particulates were pressed in a 37 mm diameter die at 70 MPa. Sintering was undertaken at 1350 °C for 8 h with consideration being given to minimise ZnO loss during this process. A cooling rate of 90 °C/h was employed (except were stated otherwise in the text) and all ceramics had >97% of theoretical density as measured using the Archimedes water immersion technique.

2.2. Quenching

Sintered samples were subsequently heated on a ZrO_2 board in a muffle furnace (ramp rate 3 °C/min) between 1100

and 1400 °C and held at temperature for 16 h. The furnace door was opened at temperature and the samples removed and dropped into water.

2.3. Characterisation

X-ray diffraction was performed on powdered samples using a Philips X-ray diffractometer. X-ray patterns were recorded at 2θ values between 10 and 80° at a scanning rate of 2° 2θ/min using non-monochromated Cu Kα radiation.

Scanning electron microscopy (SEM) was performed on fracture surfaces from quenched pellets. Samples were mounted on aluminium pin stubs using silver paste (Agar Scientific Ltd., Essex) and gold sputter coated. Secondary electron images were obtained using a JEOL 6400 SEM operating at 20 kV.

A Renishaw Ramascope System 2000 spectrometer was used for Raman measurements. This system comprised an integral Raman microscope, a stigmatic single spectrograph and a Peltier-cooled CCD detector. The microscope attachment was an Olympus BH2 system and the excitation wavelength used was 633 nm from a He–Ne laser source. Power of 1–3 mW was incident on the samples in a 2 μm diameter spot through a standard 50× microscope objective lens. The spectra were collected with 30 s data point acquisition time, a spectral range of 150–950 cm^{-1} and a spectral resolution of 3–4 cm^{-1}. Raman spectra were analysed using GRAMS/AI V.7, which is a fully interactive data processing package including peak-fitting, data smoothing, quantitative analysis, peak picking and integration for Raman spectrum analysis. Spectra were then presented as relative intensity (counts) versus Raman shift (cm^{-1} in air).

Fragments of quenched samples were also used to prepare TEM samples. Pieces, approximately 3 mm diameter, were mounted on a Gatan disc grinder stub using Crystalbond 'heat on/heat off' resin. The ceramic was ground flat on one side using the Gatan disc grinder, removed from the Gatan disc grinder stub and remounted with the flat side down. The sample was further ground to approximately 20 μm thick and a 3.05 mm Cu support ring with 800 μm circular hole was glued onto its surface using an epoxy resin. The sample was removed from the stub and excess Crystalbond cleaned off its surface using acetone. The samples were thinned in a Gatan Duo Mill ion beam thinner operating at an accelerating voltage of 6 kV and a combined gun current of 0.6 mA at an incidence angle of 15°. The samples were examined using a JEOL 3010 and Philips Tecnai TEM's operating at an accelerating voltage of 300 and 200 kV, respectively.

3. Results

3.1. SEM and XRD

Fig. 1 shows typical secondary electron SEM images of fractured BCZN–BGT samples annealed and quenched from (a) 1100 °C, (b) 1200 °C, (c) 1300 °C and (d) 1400 °C. The grain size increases from ∼10 to ∼20 μm as the annealing

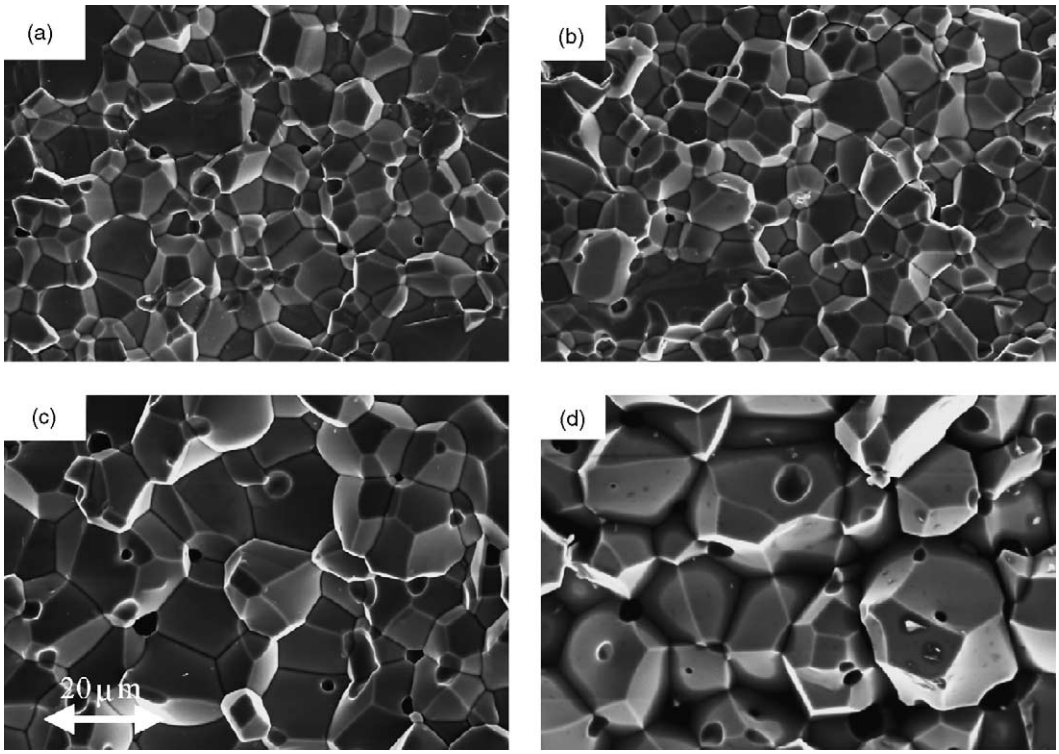

Fig. 1. Secondary electron SEM images of fractured BCZN–BGT samples annealed and quenched from (a) 1100 °C, (b) 1200 °C, (c) 1300 °C and (d) 1400 °C.

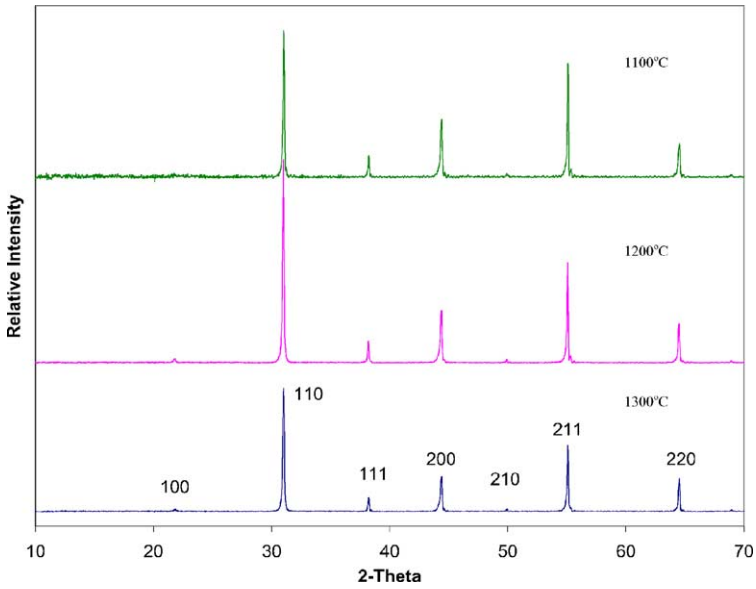

Fig. 2. XRD patterns from sintered BCZN–BGT ceramics annealed and quenched from 1100, 1200 and 1300 °C.

temperature is increased from 1100 to 1400 °C, respectively. Fig. 2 shows the XRD patterns from BCZN–BGT pellets, annealed and quenched from 1100, 1200 and 1300 °C, respectively. All peaks may be indexed according to a simple perovskite cell (*Pm*3*m*) with $a = 4.09$ Å, No second phase was detected and there was no evidence of superlattice reflections.

3.2. Raman spectroscopy

Fig. 3 shows the Raman spectra between 150 and 950 cm^{-1} from BCZN–BGT samples, annealed and quenched from (a) 1100 °C, (b) 1200 °C (c) 1250 °C and (d) 1300 °C. The bands marked as A_{1g} and F_{2g} are characteristic of ordering in B-site complex perovskites.[21,22] The F_{2g} mode band is only sensitive to long-range order (LRO) on the B-site whereas the A_{1g} mode band may result from either LRO or short-range order (SRO).[21,22] In general, more ordered samples exhibit narrower widths and higher intensities.[21,22] Fig. 3 reveals that samples annealed and quenched from 1100 °C exhibits LRO as evidenced by the presence of the F_{2g} band which persists up to 1200 °C. However, the degree of LRO is greatly reduced, as indicated by a much lower intensity and broader width of both

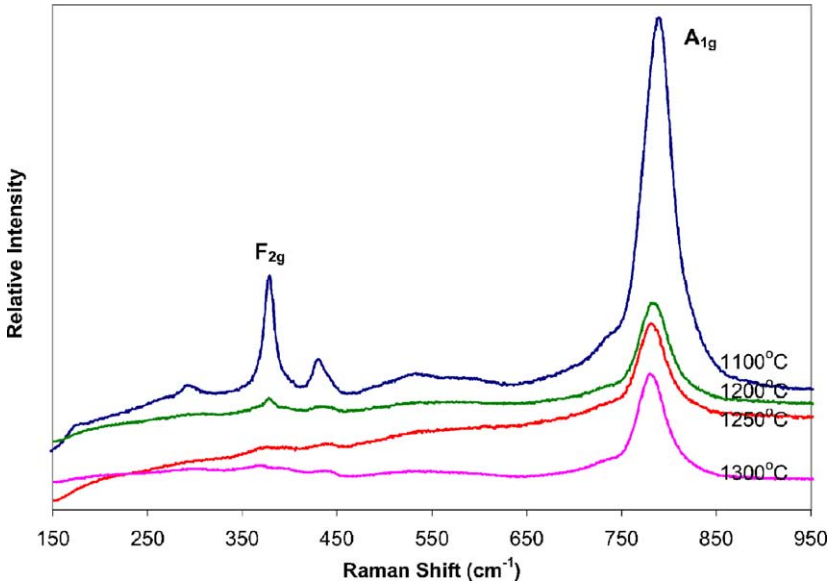

Fig. 3. Raman spectroscopy data from BCZN–BGT samples, annealed and quenched from (a) 1100 °C, (b) 1200 °C, (c) 1250 °C and (d) 1300 °C. The F_{2g} mode at ~380 cm^{-1} indicates only long range B-site order while the A_{1g} mode at ~800 cm^{-1} may be present due to both short- and long-range ordering.

the F_{2g} and A_{2g} bands. In samples annealed and quenched from 1250 and 1300 °C, the F_{2g} band is no longer visible, suggesting LRO is absent. However, the A_{1g} band is still present although its intensity is diminished and its bandwidth broader, indicating that SRO may still be present.

3.3. TEM

Fig. 4a–c are $\langle 1\,1\,0\rangle_p$ zone axis diffraction electron diffraction patterns (ZADP's) obtained, from grains in BZN–BGT ceramics, annealed and quenched from 1100, 1200 and 1300 °C, respectively. The most intense spots may be indexed according to the fundamental perovskite structure, $a_o = 4.09$ Å (from XRD data). Electron diffraction patterns recorded from samples quenched from 1100 °C (Fig. 4a) exhibited discrete superlattice reflections at all $\pm 1/3\{h\,k\,l\}_p$ and diffuse intensities at $1/2\{h\,k\,l\}_p$ positions. The appearance of $\pm 1/3\{h\,k\,l\}_p$ reflections is consistent with the presence of at least two variants (within the diffracting volume) of a trigonal supercell in which $a = b \approx 5.78$ Å, $c \approx 7.09$ Å (i.e. $a = b = \sqrt{2} \times a_o$, $c = 3 \times a_o/\sqrt{3}$). The supercell may be explained by considering that the B-site cations are ordered alternately in a 1:2 ratio on $\{1\,1\,1\}_p$ planes, e.g. $(1\,1\,1)_p$ or $(-1\,-1\,-1)_p$. This ordering sequence was initially reported by Galasso[23] as the $Ba(Sr_{1/3}Ta_{2/3})O_3$ structure whose symmetry may described by space group, $P\bar{3}m1$.[24] The presence of diffuse $1/2\{h\,k\,l\}_p$ reflections suggests that short range 1:1 ordering coexists with long range 1:2 ordered regions. In contrast, samples annealed and quenched from ≥1200 °C (Fig. 4b and c) showed only the presence of diffuse and weak superlattice intensities, which consisted of streaks parallel with $\langle 1\,1\,1\rangle_p$ directions. Where these diffuse streaks crossed at $1/2\{h\,k\,l\}_p$ positions, the intensity was enhanced to give an average short-range ordered fcc superstructure reflection. Unlike X-ray and neutron, electron diffraction intensities are difficult to quantify and use in the interpretation of structure, due to dynamic rather kinematic scattering. However, it is broadly true that diffuse intensities arise from short range interactions (1–2 nm) whereas sharp discrete reflection from long range (>3 nm). The electron diffraction data is therefore in agreement with that obtained by Raman spectroscopy.

Fig. 5a and b are two-beam bright field TEM images of a grain from samples annealed and quenched from 1100 and 1250 °C, respectively. The underlying diffraction contrast in Fig. 5a is mottled (arrowed on left hand side). Barber et al.[5] and Reaney et al.[13] have interpreted this contrast as aris-

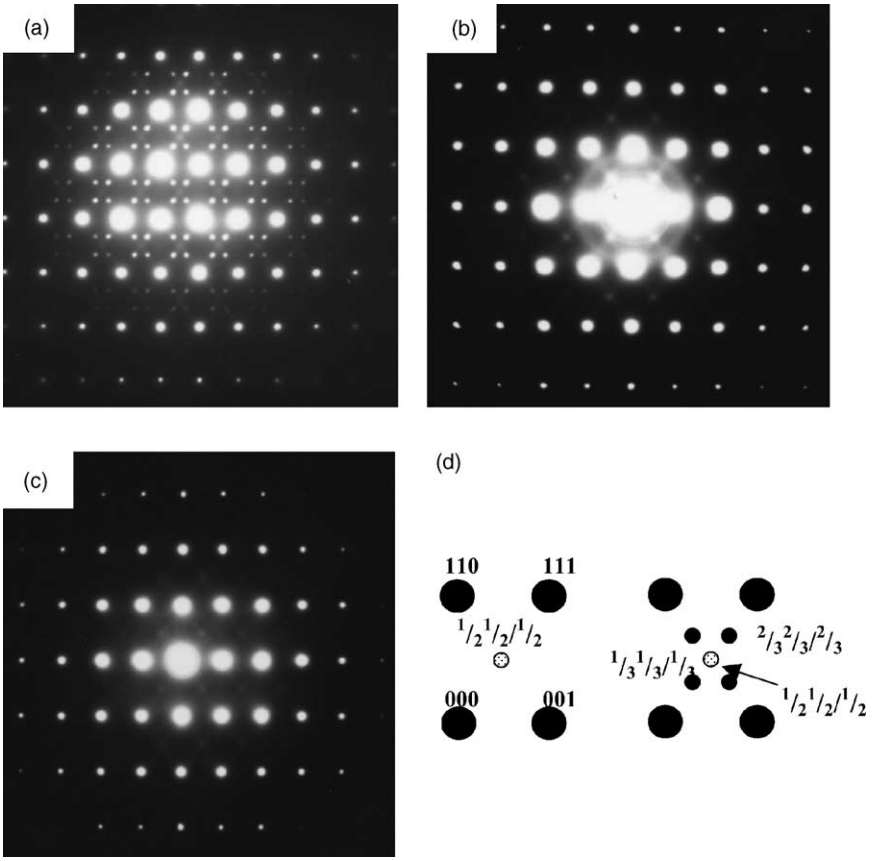

Fig. 4. (a and b) $\langle 1\,1\,0\rangle_p$ Zone axis diffraction. Electron diffraction patterns obtained, from grains in BZN–BGT ceramics, annealed and quenched from (a) 1100 °C, (b) 1200 °C and (c) 1300 °C. (d) Schematic indexing of the patterns.

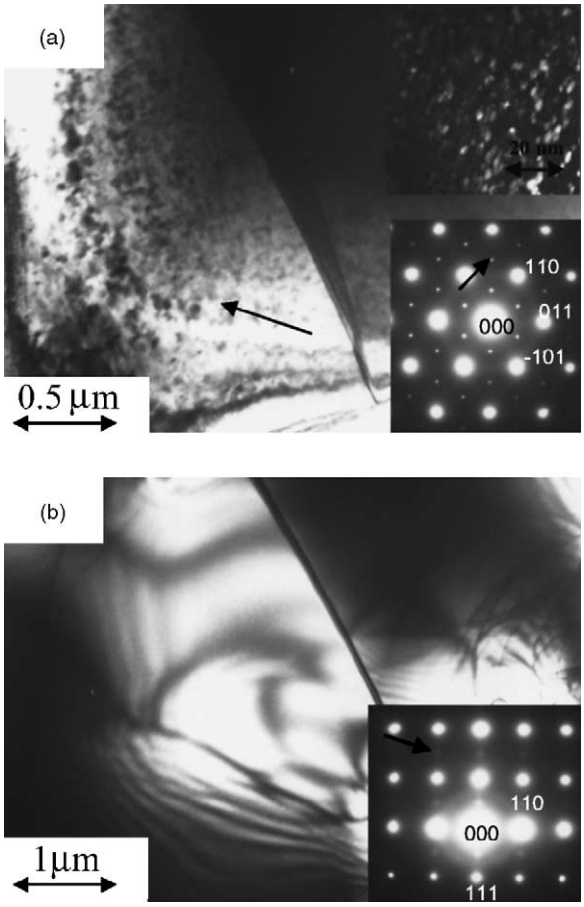

Fig. 5. (a and b) Bright field TEM images grains in samples annealed and quenched from 1100 and 1250 °C, respectively (mottled contrast is arrowed in Fig. 5a). Inset ZADPs are (a) $\langle 1\,1\,1\rangle_p$ showing $\pm 1/3\{h\,k\,l\}_p$ superlattice reflections and (b) $\langle 2\,1\,1\rangle_p$ showing diffuse $1/2\{h\,k\,l\}_p$ reflections (each are arrowed). Also inset in Fig. 5a is a dark field TEM image obtained using a $\pm 1/3\{h\,k\,l\}$ superlattice reflection. Bright contrast reveals the ordered domain distribution.

ing from strained boundaries between ordered variants of trigonal superstructure which have impinged. The ordered domains are highlighted in the dark field image (obtained using a $\pm 1/3\{h\,k\,l\}$ reflection) inset in the top right hand corner of Fig. 5a. A $\langle 1\,1\,1\rangle_p$ zone axis diffraction pattern is also inset which shows 1:2 ordered superlattice reflections at $\pm 1/3\{h\,k\,l\}_p$ positions. The strain at the ordered domain boundaries arises due to a distortion of the pseudocubic lattice in the $[1\,1\,1]_p$ direction as the B-site cations order.[11] Mottled contrast could not be obtained from samples annealed from 1250 °C and any features present in Fig. 5b are artefacts of the imaging technique rather than arising from the structure. Inset in Fig. 5b is a $\langle 2\,1\,1\rangle_p$ zone axis electron diffraction pattern which shows only diffuse superlattice reflections at $1/2\{h\,k\,l\}_p$ positions.

4. Discussion

Although no superlattice reflections could be detected by XRD, TEM and Raman spectroscopy have clearly shown that BCZN–BGT has an order–disorder phase transition at ~1200 °C. The contrast from bright and dark field images suggests that the size (10–20 nm) and distribution of ordered domains are similar in nature to those in BZT and BZT–SGT when these compounds are annealed below their order disorder phase transition temperature.[13,14] The presence of 1:2 ordered regions distributed throughout grains indicates that Co readily substitutes for Zn in the ordered trigonal supercell, defining the valence state as Co^{2+}. In addition, it is clear that the addition of 10% BGT to BCZN is insufficient to suppress completely 1:2 ordering. There is no direct evidence of any macroscopic partitioning of Ga and Ta in the grains but the coexistence of short range 1:1 with long range 1:2 ordered regions suggests that there may be a heterogeneous distribution of cations on the B-site for samples annealed and quenched from 1100 °C.

In BCZN–BGT compositions, only the BCZN component has the correct stoichiometry to form 1:2 ordered regions. If it is assumed that the BCZN component orders completely then the BGT (10 mol%, 1:1 end member compound) will partition at the interfaces between ordered regions. Davies and Tong[9] suggested that Zr partitions to the orientational domain boundaries in BZT–$BaZrO_3$ although they did not present any direct evidence to support this hypothesis. In BCZN–BGT, the residual Ga and Ta ions exist in a 1:1 ratio and have a significant charge difference. Therefore, it is feasible that they may form a short range, 1:1, fcc superstructure at the 1:2 ordered domain boundaries which could give rise to the observed $1/2\{h\,k\,l\}_p$ superstructure reflection in samples annealed and quenched from 1100 °C. As in BZT, and BZT–SGT, an average short range fcc superstructure also persists in samples quenched from above the order–disorder phase transition temperature (>1200 °C) in BCZN–BGT. However, its presence is always accompanied by streaking parallel to the $\langle 1\,1\,1\rangle_p$ directions which arise from short range 1:2 ordering.[13] It is not possible to know whether the short range fcc structure is thermodynamically stable at >1200 °C or is induced because the quench rate is insufficient to arrest fully the ordering process. Although the quenched samples could not be measured at MW frequencies due to extensive internal cracking, slow (5 °C/h) were compared with rapid (180 °C/h) furnace cooled samples. The former exhibited Raman active modes and electron diffraction patterns identical to those associated with samples quenched from 1100 °C, Figs. 3 and 4a, respectively. In contrast, rapid cooling the samples gave rise to spectra and diffraction patterns similar to those from samples quenched from 1300 °C (Figs. 3 and 4c). The Q at MW frequencies was typically 12–18,000 and 25–30,000 at the rate of 3.05 GHz for the slow and fast cooled samples, respectively. The commensurate increase of MW Q with the degree of order observed in BCZN–BGT is consistent with observations on BZT-based compositions.[3–5,9,13,14]

5. Conclusions

(1) BCZN–BGT ceramics exhibit an order–disorder phase transition at ∼1200 °C which is difficult to detect by X-ray diffraction but may be readily observed by using electron microscopy and Raman spectroscopy.
(2) Below the order disorder phase transition long range 1:2 ordered domains coexist with short range 1:1 ordered regions. It is postulated that the 1:2 ordered regions are associated with BCZN while 1:1 order mainly arises from BGT rich regions partitioned at the 1:2 domain boundaries.
(3) Above the order–disorder phase transition, short range 1:2 ordering is observed as streaks along $\langle 1\,1\,1\rangle_p$ directions. Where intensities overlap, a $1/2\{h\,k\,l\}$ reflection is observed, suggesting an average short range fcc ordered structure.

Acknowledgements

The authors are grateful to Dr. P. Korgul, Mr. H. Bagshaw and Miss F. Ahmar for help with electron microscopy.

References

1. Moulson, A. J. and Herbert, J. M., *Electroceramics*. Chapman and Hall, London, 1990.
2. Hirahara S., Fujikawa N., Enami S. and Noshi, T., U.S. Patent No 5356844, 1994.
3. Okuyama, K., Yokotani, Y. and Kugimiya, K., U.S. Patent No 5470808, 1995.
4. Nomura, S., Ceramics for microwave dielectric resonator. *Ferroelectrics* 1983, **49**, 61–70.
5. Barber, D. J., Moulding, K. M., Zhou, J. I. and Li, M., *J. Mater. Sci.* 1997, **32**, 1531–1544.
6. Shannon, R. D. and Prewett, C. T., Revised values of effective ionic radii. *Acta Cryst.* 1976, **A32**, 751.
7. Reaney, I. M., Colla, E. L. and Setter, N., *Jpn. J. Appl. Phys.* 1994, **33**(7), 3984.
8. Colla, E. L., Reaney, I. M. and Setter, N., *J. Appl. Phys.* 1993, **74**(5), 3414.
9. Davies, P. K. and Tong, J., *J. Am. Ceram. Soc.* 1997, **80**, 1727–1740.
10. Hughes, H., Iddles, D. and Reaney, I. M., *Appl. Phys. Lett.* 2001, **79**(18), 2952–2954.
11. Jacobson, A. J., Collins, B. M. and Fender, B. E. F., *Acta Cryst.* 1976, **B32**, 1083–1087.
12. Desu, S. B. and O'Bryan, H. M., *J. Am. Ceram. Soc.* 1985, **68**(10), 546–551.
13. Reaney, I. M., Qazi, I. and Lee, W. E., *J. Appl. Phys.* 2000, **88**(11), 6708–6714.
14. Reaney, I. M., Wise, P. L., Qazi, I., Miller, C. A., Price, T. J., Cannell, D. S. *et al.*, *J. Eur. Ceram. Soc.* 2003, **23**(16), 3021–3034.
15. Kageyama, K., *J. Am. Ceram. Soc.* 1992, **75**(7), 1767–1771.
16. Noh, S. Y., Yoo, M. J., Nahm, S., Choi, C. H., Park, H. M. and Lee, H. J., *Jpn. J. Appl. Phys.* 2002, **41**, 2978–2981.
17. Ahn, C. W., Nahm, S., Lim, Y. S., Choi, W., Park, H. M. and Lee, H. J., *Jpn. J. Appl. Phys.* 2002, **41**, 5277–5280.
18. Endo, K., Fujimoto, K. and Murakawa, K., *J. Am. Ceram. Soc.* 1987, **70**(9), C215–C218.
19. Iddles, D., *Internal Report on Ba Based Perovskites*. Filtronic Comtek, Wolverhampton, UK.
20. Colla, E., Reaney, I. M. and Setter, N., *J. Appl. Phys.* 1993, **74**(5), 3414–3425.
21. Siny, I. G., Tao, R. W., Katiyar, R. S., Guo, R. Y. and Bhalla, A. S., *J. Phys. Chem. Solids* 1998, **59**(2), 181–195.
22. Burns, G. and Scott, B. A., *Solid State Commun.* 1973, **13**, 423.
23. Galasso, F. S., *Stucture Properties and Preparation of Perovskite Type Compounds*. Pergamon Press, Oxford, London, 1969.
24. Jacobson, A. J., Collins, B. M. and Fender, B. E. F., *Acta Cryst.* 1976, **B32**, 1083–1087.